

Intersystem Crossing to Excited Triplet State of Aza Analogues of Nucleic Acid Bases in Acetonitrile

Takashi Kobayashi, Hikaru Kuramochi, Yosuke Harada, Tadashi Suzuki,* and Teijiro Ichimura

Department of Chemistry and Materials Science, Tokyo Institute of Technology, 2-12-1 Ohokayama, Meguro-ku, Tokyo 152-8551, Japan

Received: June 10, 2009; Revised Manuscript Received: September 7, 2009

Excited state characteristics of aza analogues of nucleic acid bases, 8-azaadenine (8AA), 5-azacytosine (5AC), 8-azaguanine (8AG), and 6-azauracil (6AU), in acetonitrile solution were comprehensively investigated with steady state absorption and emission spectra, transient absorption measurements, emission measurements for the singlet oxygen molecule, and time-dependent density functional theory (TD-DFT) calculations. The triplet–triplet absorption spectrum of 8AA whose peak was 455 nm was observed for the first time. Sensitized singlet oxygen formation of 8AA was also observed in O₂-saturated acetonitrile with quantum yields of 0.15 ± 0.02. It was concluded that there were two kinds of aza analogues of nucleic acid bases: type A had substantial quantum yield for the intersystem crossing and potential of O₂ (¹Δ_g) formation (8AA and 6AU), and type B did not (5AC and 8AG). TD-DFT calculations indicated that type A molecules had a dark ¹nπ* state below the first allowed ¹ππ* state, while both S₁ and S₂ states for type B molecules had a ππ* character. It strongly suggested that the dark ¹nπ* state below the ¹ππ* state would play an important role in the ISC process of aza analogues of nucleic acid bases.

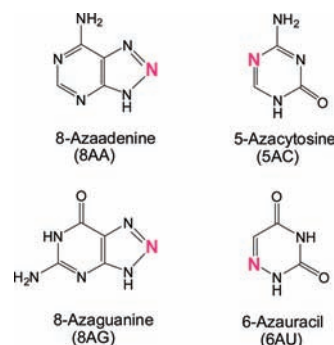
Introduction

Nucleic acid bases (adenine, cytosine, guanine, thymine, and uracil) serve as a main chromophore of DNA and RNA absorbing radiation below 300 nm.¹ Light absorption by nucleic acid bases will cause lethal photodamage to DNA. To understand such phenomena fundamentally, much research with ultrafast spectroscopy and quantum chemical calculations has been carried out on the excited state dynamics of nucleic acid bases in recent years.^{2–14} In general, nucleic acid bases are extremely stable to photochemical reaction, because the bases in the excited singlet states exhibit a remarkably rapid decay into the ground (S₀) state.^{2–4}

It was clarified in our previous works that the relaxation dynamics of nucleic acid bases was quite sensitive to some chemical substitutions.^{15,16} In particular, the excited state dynamics of 6-azauracil (6AU, Chart 1), which has an N atom inserted into the C6 of uracil, was studied in acetonitrile.¹⁶ It was found to drastically differ from that of uracil: high yields for intersystem crossing (ISC) (1.00 ± 0.10) and the singlet oxygen O₂ (¹Δ_g) formation (0.63 ± 0.03) with 248 nm excitation. The N substitution resulted in a change of dominant relaxation processes of uracil from ultrafast internal conversion to ultrafast ISC. Although there were some cases in which an N substitution results in a change of relaxation processes like the case of benzene and pyridine,^{17,18} our results were quite an interesting report in terms of changing intrinsic ultrafast internal conversion of nucleic acid bases with a simple chemical modification. Investigation of other aza analogues of nucleic acid bases will give us meaningful information on potential energy surfaces including conical intersections, which have been studied extensively^{2–14} on the relaxation process of normal nucleic acid bases.

In this work, 8-azaadenine (8AA), 5-azacytosine (5AC), 8-azaguanine (8AG), and 6AU were comprehensively investi-

CHART 1: Molecular Structures of Aza Analogues of Nucleic Acid Bases



gated (Chart 1). 8AA has been used in the treatment of cancer,¹⁹ asthma, and allergenic diseases.^{20,21} 5AC and 8AG are known to have a cancerostatic^{22,23} and antineoplastic effect.²⁴ Under medical cancer treatment with the aza analogues, chemotherapy and photodynamic therapy are often performed simultaneously; however, photosensitivity was also reported.^{25,26} Knowledge of the excited state characteristics of the aza-substituted nucleic acid bases is of great importance and is very meaningful. In this article, the excited state characteristics of 8AA, 5AC, and 8AG in acetonitrile were investigated by means of steady state absorption and emission spectra measurements, laser flash photolysis, emission measurements for the singlet oxygen molecule, and time-dependent density functional theory (TD-DFT) calculations. In acetonitrile, a polar but aprotic solvent, we could exclude the formation of solute/solvent hydrogen bonds and the influence of the photoreaction such as the addition of a water molecule,²⁷ and we could investigate the intrinsic excited state dynamics of the aza analogues of nucleic acid bases.

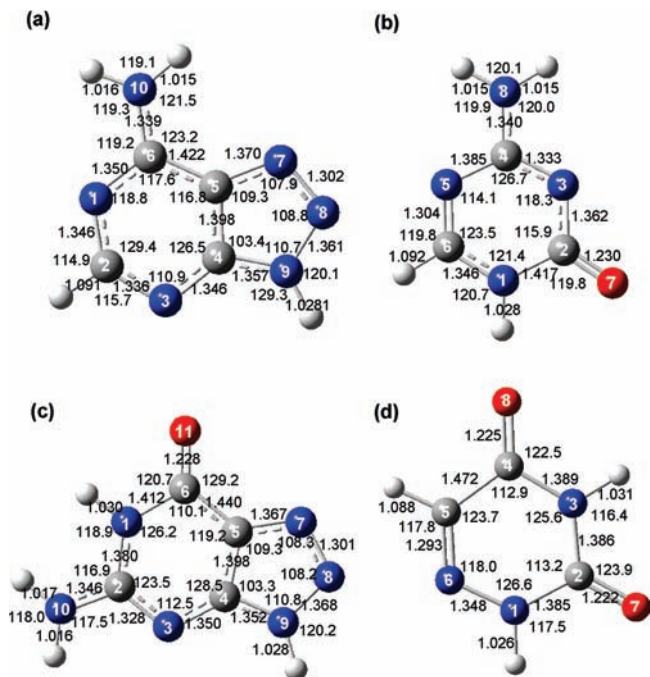


Figure 1. Optimized molecular structures, the bond lengths (Å), and the angles (deg) of (a) 8AA, (b) 5AC, (c) 8AG, and (d) 6AU.

Experimental Section

Materials. 5AC, 6AU, 8AA, 8AG, adenine, cytosine, guanine, and uracil were purchased from Sigma Aldrich and used without further purification. Acetonitrile (Kanto Chemical, GR grade) was used from a freshly opened bottle. Sample solutions were deaerated by bubbling with Ar gas or flashed with O₂ gas for 30 min.

Apparatus. For the transient absorption measurement, a KrF excimer laser (Lambda Physik, COMPex102; 248 nm, 350 mJ/pulse, 30 ns pulse duration) was used as an excitation light source and a Xe flash lamp (Ushio UXL-300DO; 300 W) was used as a monitoring light source.

The spectra of the emission of singlet oxygen, O₂ (¹Δ_g), were measured by using a time-correlated single photon counting apparatus (Hamamatsu Photonics, C7990) with a Nd³⁺:YAG laser light operated at 266 nm (CryLas, FQSS266-Q2; 2.8 μJ/pulse, <1 ns pulse duration, repetition rate = 3 kHz) as an excitation source. The overall instrumental response function was about 400 ps. The emission quantum yield of O₂ (¹Δ_g) was determined with an InGaAs PIN photodiode (Hamamatsu Photonics G8376-05) and a handmade amplifier. Since the InGaAs PIN photodiode has spectral sensitivity for the wavelength region of 1100–1400 nm, it can be applied to the observation of the luminescence from O₂ (¹Δ_g).^{16,28,29}

The sample solution flowed into the cuvette to remove the influence of photoproducts. All the measurements were carried out at room temperature.

The UV absorption spectrum was measured with a double beam spectrometer (Jasco Ubest V-550). The emission spectrum was measured with a spectrofluorometer (Jasco FP-6500).

Theoretical Calculation. Becke's three-parameter hybrid functional and Lee–Yang–Parr correlation functions (B3LYP) were adopted. A 6-31G(d,p) basis set was used for the geometry optimization calculations. Vertical transition energies and oscillator strengths of the excited singlet and the triplet states of aza analogues were calculated by TD-DFT, using the optimized geometry of the S₀ state. The solvent effect was computed using

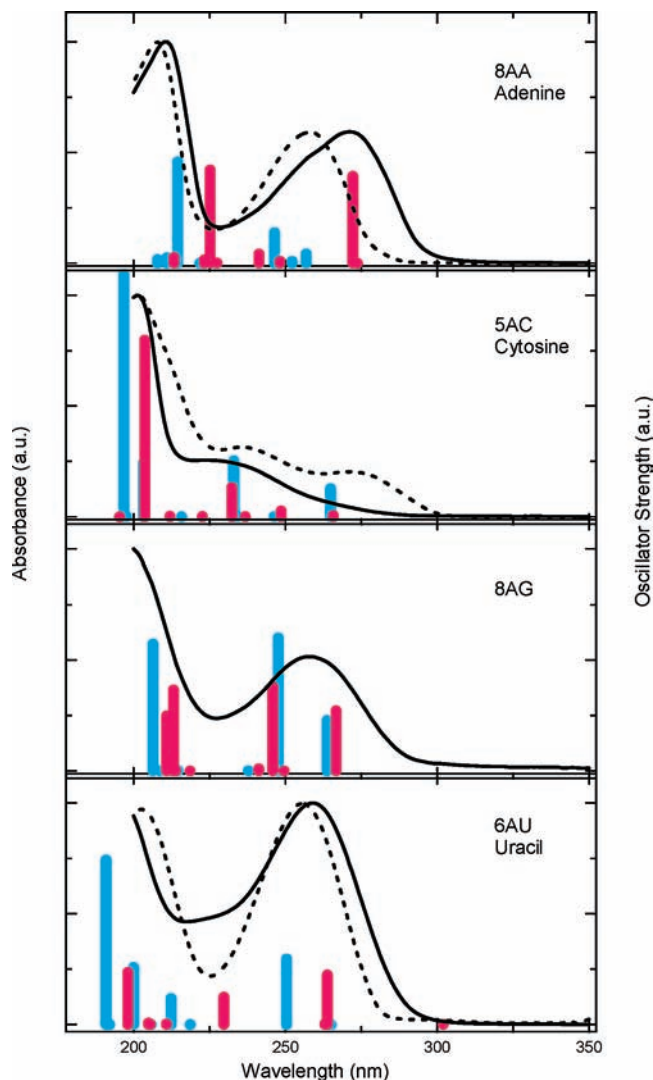


Figure 2. Absorption spectra of aza analogues of nucleic acid bases (solid line) and normal nucleic acid bases (dotted line) in acetonitrile. Computed oscillator strengths of aza analogues of nucleic acid bases (red) and normal nucleic acid bases (blue) in acetonitrile are also shown.

the polarized continuum model (PCM).^{30,31} The GAUSSIAN 03 suite of programs³² was used for the calculations. The molecular orbitals were viewed using GAUSSVIEW.³³

Results and Discussion

Molecular Structures and Electronic Configurations of Aza Analogues of Nucleic Acid Bases. The optimized ground state geometries of aza analogues of nucleic acid bases in acetonitrile are shown in Figure 1. The bond lengths and the angles for the molecules are also shown. Our calculation indicated that the S₀ state of all the aza analogues had a planar molecular structure as well as the corresponding normal bases. The molecule structures of 7-methyl-8-azaadenine,³⁴ 8AA monohydrated,³⁵ and 6AU³⁶ were reported to be planar by the X-ray structure analysis.

To investigate the electronic structures of the aza analogues, absorption spectrum measurements and TD-DFT calculations were carried out. Figure 2 shows absorption spectra of aza analogues of nucleic acid bases. For comparison, the absorption spectra of the corresponding normal nucleic acid bases except guanine (because guanine hardly dissolves in acetonitrile) are

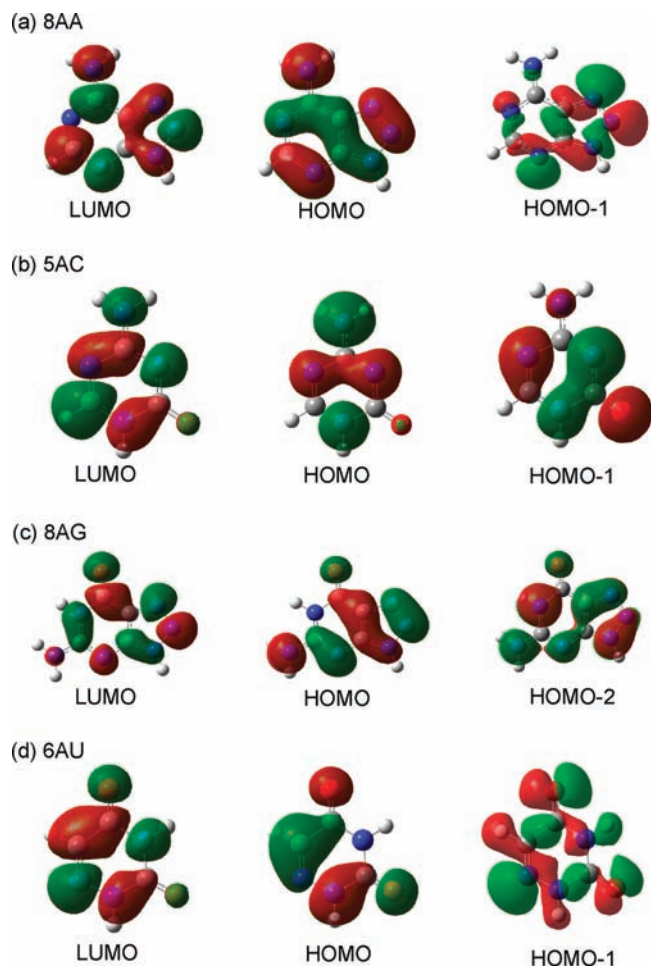
TABLE 1: Ground State Absorption Spectrum, Computed Vertical Excitation Energies (E_{calc}), and Oscillator Strengths (f_{calc}) of Excited Singlet and Triplet States of 8AA, 5AC, 8AG, and 6AU in Acetonitrile

state	nature	$\lambda_{\text{max}}^a/\text{nm}$ (cm^{-1})	$E_{\text{calc}}^{b,c}/\text{nm}$ (cm^{-1})	f_{calc}^b
8AA				
S ₁	$n\pi^*$		273 (36 540)	0.0001
S ₂	$\pi\pi^*$	275 (36 360)	272 (36 740)	0.2144
S ₃	$n\pi^*$		248 (40 300)	0.0046
S ₄	$\pi\pi^*$	257 (38 910)	241 (41 460)	0.0228
T ₁	$\pi\pi^*$		396 (25 250)	
T ₂	$n\pi^*$		304 (32 940)	
T ₃	$\pi\pi^*$		281 (35 560)	
T ₄	$\pi\pi^*$		280 (35 710)	
5AC				
S ₁	$\pi\pi^*$		266 (28 120)	0.0034
S ₂	$\pi\pi^*$	260 (38 520)	248 (40 230)	0.0145
S ₃	$n\pi^*$		237 (42 250)	0.0007
S ₄	$n\pi^*$, $\pi\pi^*$	225 (44 510)	232 (43 050)	0.0716
T ₁	$\pi\pi^*$		308 (32 490)	
T ₂	$n\pi^*$		301 (33 230)	
T ₃	$\pi\pi^*$, $n\pi^*$		285 (35 150)	
T ₄	$n\pi^*$		259 (38 740)	
8AG				
S ₁	$\pi\pi^*$	258 (38 760)	267 (37 500)	0.1482
S ₂	$\pi\pi^*$		249 (40 080)	0.0001
S ₃	$\pi\pi^*$	230 (43 570)	246 (40 690)	0.2075
S ₄	$n\pi^*$		241 (41 470)	0.0057
T ₁	$\pi\pi^*$		373 (26 800)	
T ₂	$n\pi^*$		305 (32 800)	
T ₃	$\pi\pi^*$		288 (34 710)	
T ₄	$n\pi^*$		271 (36 940)	
6AU				
S ₁	$n\pi^*$		302 (33 120)	0.0003
S ₂	$\pi\pi^*$	259 (38610)	264 (37 910)	0.1221
S ₃	$n\pi^*$		263 (38 020)	0.0016
S ₄	$\pi\pi^*$	229 (43670)	230 (43 530)	0.0674
T ₁	$\pi\pi^*$		413 (24 190)	
T ₂	$n\pi^*$		348 (28 700)	
T ₃	$\pi\pi^*$		294 (34 070)	
T ₄	$n\pi^*$		287 (34 830)	

^a The peak wavelengths of absorption spectra. ^b Calculated by the TD-DFT method for the molecular structure in the S_0 state optimized at the B3LYP/6-31G(d,p) level. ^c The values scaled by 0.95.

also shown. Oscillator strengths for each transition were calculated (see Figure 2). 8AA and 6AU had a relatively intense absorption band around 270 nm. Compared with the corresponding band of adenine and uracil, the band was red-shifted. 5AC had no absorption band peak at around 275 nm while cytosine did. Wavelengths at absorption peak maxima, computed vertical excitation energies, and oscillator strengths of excited singlet and triplet states for 8AA, 5AC, 8AG, and 6AU in acetonitrile are summarized in Table 1.

Figure 3 shows the molecular orbitals (MOs) of the aza analogues. For 8AA, the lone pair orbital of N8 contributed to the HOMO - 1, and for 6AU, that of N6 contributed to the HOMO - 1. The S_1 state of 8AA arose mainly from the HOMO - 1 \rightarrow LUMO transition, which had a $n\pi^*$ character, whereas the S_2 state predominantly had the HOMO \rightarrow LUMO transition, which had a $\pi\pi^*$ character. Similarly, 6AU had the $n\pi^*$ state below the first allowed $^1\pi\pi^*$ state, and it arose mainly from the HOMO - 1 \rightarrow LUMO transition.¹⁶ Gas-phase photoelectron spectroscopic¹¹ and theoretical¹² studies suggested that adenine had a $^1n\pi^*$ state below the first allowed $^1\pi\pi^*$ state. The $^1n\pi^*$ state of 8AA and 6AU should locate below the first allowed

**Figure 3.** Description of molecular orbitals involved in the S_1 and S_2 electronic transitions for (a) 8AA, (b) 5AC, (c) 8AG, and (d) 6AU.

$^1\pi\pi^*$ state as shown by our computational results (see Table 1), although they were not observed in the absorption spectrum due to their low oscillator strengths ($f_{\text{calc}} \approx 10^{-4}$).

Both of the S_1 and S_2 states of 5AC and 8AG had a $\pi\pi^*$ character. The S_1 state of 5AC arose mainly from the HOMO - 1 \rightarrow LUMO transition, while the corresponding state of cytosine arose mainly from the HOMO \rightarrow LUMO transition. The oscillator strengths (0.0034 for 5AC and 0.0692 for cytosine) were consistent with the absorption intensities for 5AC and cytosine. The S_2 state of 5AC arose mainly from the HOMO \rightarrow LUMO transition. The S_1 state of 8AG arose mainly from the HOMO \rightarrow LUMO transition, and the S_2 state predominantly has the HOMO - 2 \rightarrow LUMO transition (HOMO - 1 of 8AG was an n-type orbital, and data are not shown).

The emission spectra of 8AA, 5AC, and 8AG were measured with 248 nm excitation at room temperature. Emissions of 8AA and 8AG are shown in Figure 4. The excitation spectra are also shown in Figure 4. The spectrum of 8AA was identical to the absorption spectrum. The Φ_F value of 8AA with 248 nm irradiation was estimated to be $(3.2 \pm 0.4) \times 10^{-3}$ in comparison with naphthalene as a reference ($\Phi_F = 0.21^{37}$). The Φ_F value of 8AA in water was reported to be 8×10^{-3} ,³⁸ thus, it was the same order as the value we determined. On the other hand, the excitation spectrum of 8AG was clearly different from the absorption spectrum (Figure 4). It was also reported that the principal N(9)H tautomer was nonfluorescent ($\Phi_F < 10^{-3}$) but the N(8)H tautomer emitted fluorescence in the aqueous

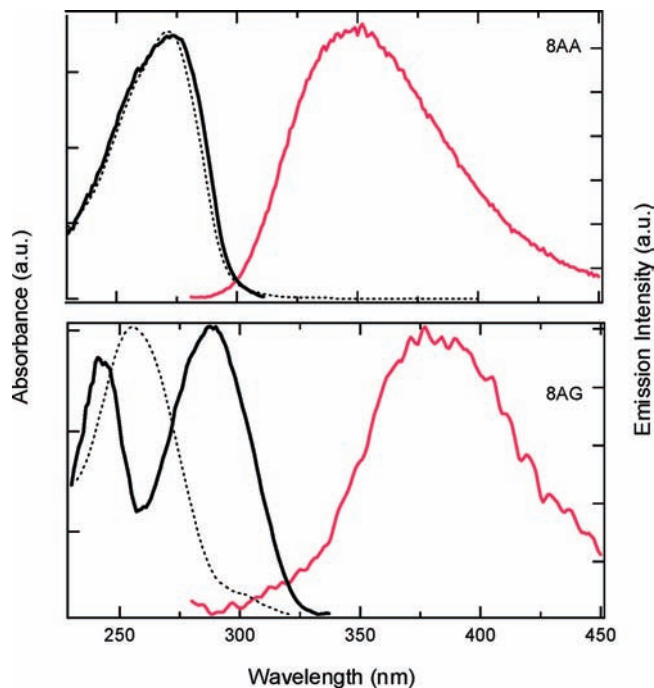


Figure 4. Absorption (dotted line), emission (red line), and excitation (black line) spectra of 8AA and 8AG in acetonitrile at room temperature. Excitation wavelength for both emission spectra was 248 nm, and monitoring wavelengths for the excitation spectra of 8AA and 8AG were 350 and 380 nm, respectively.

solution.³⁸ The fluorescent species would be N(8)H tautomer because the excitation spectrum was similar to the reported one for the N(8)H tautomer in aqueous solution. No emission of 8AG and 5AC was observed with the 248 nm excitation at room temperature, revealing that the Φ_F value of 8AG and 5AC from the excited singlet state to the S_0 state was quite low ($<10^{-3}$).

Transient Absorption Measurement of Aza Analogues of Nucleic Acid Bases. To obtain the spectral and kinetic information on excited states for the aza analogues of nucleic acid bases, 8AA, 5AC, and 8AG, laser flash photolysis was utilized to measure transient absorption spectra. Figure 5a shows the transient absorption spectrum of 8AA in Ar-saturated acetonitrile obtained immediately after the 248 nm laser irradiation. An absorption peak was observed at around 455 nm. Figure 5b shows the time profiles of the transient absorption at 455 nm under Ar saturation or aerated conditions. The absorption decayed with the first-order kinetics, and the decay rate constant was estimated to be $(4.3 \pm 0.1) \times 10^6 \text{ s}^{-1}$. The rate constant did not depend on the monitoring wavelength. The decay rate constant was estimated to be $(2.0 \pm 0.1) \times 10^7 \text{ s}^{-1}$ in the aerated acetonitrile solution. The spectrum obtained under the aerated condition corresponded to that in the Ar-saturated solution, but the lifetime of the transient became shorter. As the transient had a lifetime for submicrosecond order and it was effectively quenched by O_2 , the spectrum was assigned to the absorption of $^38AA^*$. The information on triplet 6AU has been already shown in our previous report; the peak wavelength of the triplet–triplet (T–T) absorption was 320 nm, and the triplet lifetime was 190 ns in the Ar-saturated acetonitrile.

Transient absorption spectra of 5AC and 8AG were also measured. A very weak and broad band was observed in the region from 300 to 700 nm (data not shown). However, since they were not quenched by dissolved O_2 molecules, the transient species were not $^55AC^*$ and $^88AG^*$. These results reveal that 5AC and 8AG should have a quite low triplet yield.

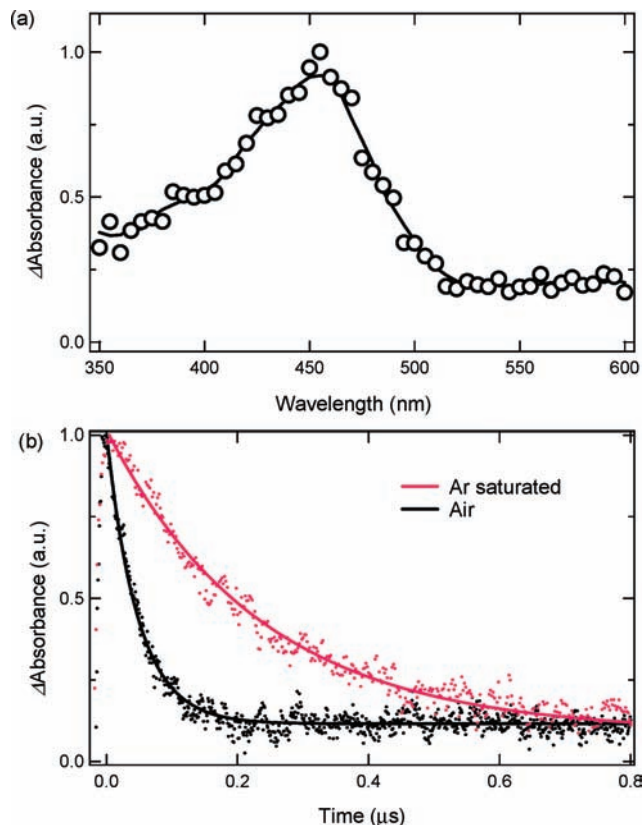
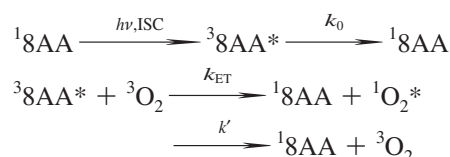


Figure 5. (a) Transient absorption spectrum of 8AA in Ar-saturated acetonitrile obtained immediately after the 248 nm laser irradiation. (b) Time profiles of the transient absorption of 8AA monitored at 455 nm in Ar-saturated (red) and air-saturated (black) acetonitrile. The solid lines denote the analytical results obtained with the single-exponential equations.

Singlet Oxygen Formation by Photosensitization of Triplet 8AA. Since $^38AA^*$ was quenched by dissolved molecular oxygen, a sensitization reaction between $^38AA^*$ and molecular oxygen should occur



where k_0 is the unimolecular decay rate constant of $^38AA^*$ in the absence of 3O_2 , k_{ET} is the bimolecular quenching rate constant of $^38AA^*$ by 3O_2 with energy transfer, and k' is the bimolecular quenching rate constant without energy transfer. To confirm the existence of the $O_2(^1\Delta_g)$ molecule by photosensitization by $^38AA^*$, the emission spectrum was observed in the near IR region by means of the time-correlated single photon counting method. Figure 6 shows the emission spectrum observed upon excitation of 8AA in air-saturated acetonitrile in the near IR region after the 266 nm laser irradiation. An emission band was observed with a maximum in the vicinity of 1270 nm, indicating that the emission band was ascribable to the phosphorescence of $O_2(^1\Delta_g)$.

The yield (Φ_Δ) of $O_2(^1\Delta_g)$ photosensitized by $^38AA^*$ was determined with the InGaAs PIN photodiode under the O_2 -saturated condition in acetonitrile. Figure 7 shows the Φ_Δ values of the aza analogues of nucleic acid bases in O_2 -saturated acetonitrile with the 248 nm excitation obtained with 6AU (Φ_Δ

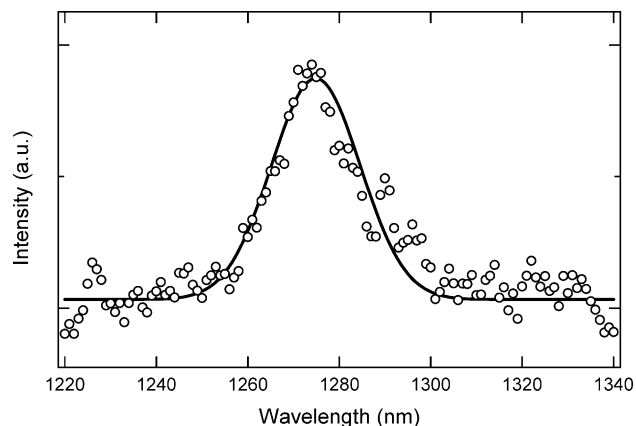


Figure 6. Luminescence spectrum of 8AA (black) in air-saturated acetonitrile obtained by the 266 nm laser irradiation. The solid line designates the best fit line obtained with the Gauss function.

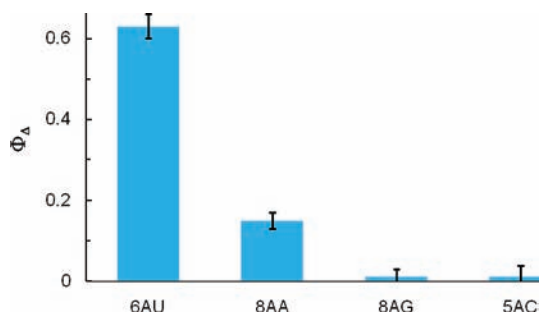


Figure 7. Quantum yield for the $O_2(^1\Delta_g)$ of aza analogues of nucleic acid bases in O_2 -saturated acetonitrile obtained with the 248 nm laser irradiation.

$= 0.63)^{16}$ as a reference. Only 8AA showed a significant Φ_{Δ} value (0.15 ± 0.02). The Φ_{Δ} values of 5AC and 8AG were negligibly low ($<10^{-2}$). These results also indicate that the Φ_{ISC} values of 5AC and 8AG are quite low.

Intersystem Crossing of Aza Analogues of Nucleic Acid Bases. Our experimental results indicate that there are two kinds of the aza analogues. One is the type which has a substantial value of Φ_{ISC} and potential of $O_2(^1\Delta_g)$ formation by photosensitization from the excited triplet state (8AA and 6AU: type A). Another one is the type which should have a quite low Φ_{ISC} value (5AC and 8AG: type B). This type of molecule cannot generate a significant amount of $O_2(^1\Delta_g)$.

Figure 8 shows the vertical transition energies from the S_0 state of the aza analogues of nucleic acid bases. From our calculations, all four aza analogues of nucleic acid bases were excited to the allowed $\pi\pi^*$ state by the 248 nm irradiation. Type

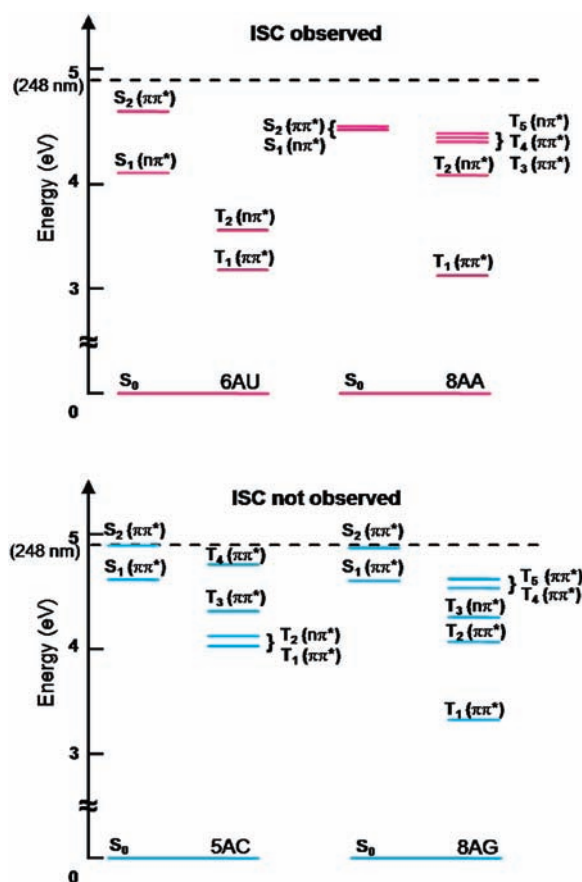


Figure 8. Computed vertical excitation energies of the lower singlet (S_n) and triplet states (T_n) for the aza analogues of nucleic acid bases in acetonitrile.

A molecules had a dark ${}^1n\pi^*$ state below the first allowed ${}^1\pi\pi^*$ state, while both S_1 and S_2 states of type B molecules were $\pi\pi^*$ state. Type A molecules showed their triplet formation, and type B molecules did not. It indicates that the dark ${}^1n\pi^*$ state below the ${}^1\pi\pi^*$ state plays an important role in the ISC process of these molecules.

Rapid ISC from the $S_2(\pi\pi^*)$ to the $S_1(n\pi^*)$ state was proposed in our previous study of 6AU.¹⁶ Additionally, theoretical study using the state-averaged CASSCF method for 6AU suggested that the optimized structures at both ${}^1\pi\pi^*/{}^1n\pi^*$ conical intersection and ${}^1n\pi^*/{}^3\pi\pi^*$ crossing point are almost planar while that of ${}^1\pi\pi^*/{}^3n\pi^*$ crossing point is nonplanar.³⁹ Since 6AU at the Franck–Condon region in the ${}^1\pi\pi^*$ state has a planar structure, it would be easy to reach the ${}^1n\pi^*/{}^3\pi\pi^*$ crossing point without

TABLE 2: Photophysical Properties of 8AA, 6AU, 5AC, 8AG, and Uracil

	λ_{max}^a/nm	$k_0^b/10^6 s^{-1}$	τ_1^c/ns	$k_q^d/10^9 dm^3 mol^{-1} s^{-1}$	Φ_{ISC}^e	$\Phi_F^f \times 10^3$	Φ_{Δ}^g	S_{Δ}^h	ref
8AA	455	4.3 ± 0.1	240 ± 5	8.2 ± 0.4	—	3.2 ± 0.4	0.15 ± 0.02	—	this work
6AU	320	5.3 ± 0.2	190 ± 10	2.5 ± 0.1	1.00 ± 0.10	N.D.	0.63 ± 0.03	0.8	ref 16
uracil	340	0.70 ± 0.02^{ij}	1400 ± 100^j	6.3 ± 0.1^j	0.21 ± 0.02^j	0.035^k	0.15 ± 0.02	0.8	this work, refs 8 and 16
5AC			N.D.			N.D.	<0.01		this work
8AG			N.D.			98 ± 11^l	<0.01		this work

^a Peak wavelength of T–T absorption. ^b Rate constant of the triplet unimolecular decay. ^c Triplet lifetime ($1/k_0$). ^d Bimolecular quenching rate constant of the triplet by oxygen. The O_2 concentration of the sample solution was estimated by the literature value.⁴⁰ ^e Quantum yield for singlet \rightarrow triplet ISC. ^f Quantum yield for the fluorescence. ^g Quantum yield for generation of $O_2(^1\Delta_g)$ via photosensitization under the O_2 -saturated condition. ^h The fraction of triplet state molecule quenched by ground state oxygen that results in the formation of $O_2(^1\Delta_g)$. ⁱ The self-quenching of triplet uracil by the parent molecule in the ground state was reported. This unimolecular decay rate constant of triplet uracil was estimated with the T–T absorption decay rate constant, the rate constant of the self-quenching ($2.0 \times 10^9 dm^3 mol^{-1} s^{-1}$),⁴¹ and the concentration of uracil ($1.5 \times 10^{-4} mol dm^{-3}$). ^j Reference 16. ^k Reference 8. ^l The fluorescent species would be N(8)H tautomer. This value is lower limit because the equilibrium constant of 8AG and N(8)H tautomer in acetonitrile has not been determined. See text for details.

notable out-of-plane distortion. Blancafort reported that $^1n\pi^*$ state adenine populated via internal conversion from $^1\pi\pi^*$ state could undergo ISC to the $^3\pi\pi^*$ state.¹² In the case of 8AA, it is also likely that the $^1n\pi^*$ state below the $^1\pi\pi^*$ state plays an important role in the triplet formation.

These experimental and computational results indicate that an analysis of electronic structure is important to understand relaxation processes of the aza analogues as well as the normal nucleic acid bases. For a more detailed discussion of their relaxation mechanisms, information on vicinity and intersection between the potential energy surfaces should be required. Our results will be a clue to understanding the ultrafast relaxation of nucleic acid bases.

Conclusion

Table 2 summarizes the photophysical properties of 8AA, 5AC, 8AG, and 6AU in acetonitrile. For comparison, the photophysical properties of uracil are also shown. In this work, excited state characteristics of 8AA, 8AG, 5AC, and 6AU were investigated to obtain comprehensive knowledge about aza analogues of nucleic acid bases. Their electronic structures were investigated by absorption spectrum measurements and TD-DFT calculations. Emission of 8AA was observed, and the quantum yield of fluorescence with 248 nm irradiation was estimated to be $(3.2 \pm 0.4) \times 10^{-3}$. Transient absorption measurement and the T–T absorption spectrum of 8AA were observed for the first time with the maximum absorption peak at 455 nm. Sensitized singlet oxygen formation of 8AA was also observed in O₂-saturated acetonitrile with quantum yields of 0.15 ± 0.02 . On the other hand, the triplet and sensitized singlet oxygen formation of 5AC and 8AG was not observed.

From our results, it was clarified that there are two kinds of aza analogues of nucleic acid bases. Type A has a substantial value of Φ_{ISC} and potential of O₂ ($^1\Delta_g$) formation by photosensitization from the excited triplet state (8AA and 6AU), and type B has a negligibly low Φ_{ISC} value (5AC and 8AG). Type A molecules have a dark $^1n\pi^*$ state below the first allowed $^1\pi\pi^*$ state, while both S₁ and S₂ states of type B molecules are $\pi\pi^*$ state. It indicates that the dark $^1n\pi^*$ state below the $^1\pi\pi^*$ state plays an important role in the ISC process of these molecules.

These experimental and computational results indicate that an analysis of electronic structure is important to understand relaxation processes of analogues of nucleic acid bases. Our results will be very important information on relaxation mechanisms of not only aza analogues but also normal nucleic acid base.

Acknowledgment. We thank Hamamatsu Photonics Co., Ltd. for the emission spectra measurements of singlet oxygen by the time-correlated single photon counting system (C7990). The present work was financially supported in part by a Grant-in-Aid for Scientific Research (KAKENHI) on Priority Areas [477] “Molecular Science for Supra Functional Systems” from the Ministry of Education, Culture, Sports, Science and Technology (MEXT), Japan.

References and Notes

- (1) Favre, A. In *Bioorganic Photochemistry: Photochemistry and the Nucleic Acids*; Morrison, H., Ed.; Wiley: New York, 1990.
- (2) Crespo-Hernández, C. E.; Cohen, B.; Hare, P. M.; Kohler, B. *Chem. Rev.* **2004**, *104*, 1977.
- (3) Saigusa, H. *J. Photochem. Photobiol., C* **2006**, *7*, 197.

- (4) Middleton, C. T.; Harpe, K. d. L.; Su, C.; Law, Y. K.; Crespo-Hernández, C. E.; Kohler, B. *Annu. Rev. Phys. Chem.* **2009**, *60*, 217.
- (5) Matsika, M. *J. Phys. Chem. A* **2004**, *108*, 7584.
- (6) Zgierski, M. Z.; Patchkovskii, S.; Fujiwara, T.; Lim, E. C. *J. Phys. Chem. A* **2005**, *109*, 9384.
- (7) Gustavsson, T.; Sarkar, N.; Lazzarotto, E.; Markovitsi, D.; Improta, R. *Chem. Phys. Lett.* **2006**, *429*, 551.
- (8) Gustavsson, T.; Bányász, A.; Lazzarotto, E.; Markovitsi, D.; Scalmani, G.; Frisch, M. J.; Barone, V.; Improta, R. *J. Am. Chem. Soc.* **2006**, *128*, 607.
- (9) F.; Barone, V.; Gustavsson, T.; Improta, R. *J. Am. Chem. Soc.* **2006**, *128*, 16312.
- (10) So, R.; Alavi, S. *J. Comput. Chem.* **2007**, *28*, 1776.
- (11) Ullrich, S.; Schultz, T.; Zgierski, M. Z.; Stolow, A. *J. Am. Chem. Soc.* **2004**, *126*, 2262.
- (12) Blancafort, L. *J. Am. Chem. Soc.* **2006**, *128*, 210.
- (13) He, Y.; Wu, C.; Kong, W. *J. Phys. Chem. A* **2003**, *107*, 5145.
- (14) He, Y.; Wu, C.; Kong, W. *J. Phys. Chem. A* **2004**, *108*, 943.
- (15) Harada, Y.; Suzuki, T.; Ichimura, T.; Xu, Y.-Z. *J. Phys. Chem. B* **2007**, *111*, 5518.
- (16) Kobayashi, T.; Harada, Y.; Suzuki, T.; Ichimura, T. *J. Phys. Chem. A* **2008**, *112*, 13308.
- (17) Quina, F. H.; Carroll, F. A. *J. Am. Chem. Soc.* **1976**, *98*, 6.
- (18) Yamazaki, I.; Sushida, K.; Baba, H. *J. Chem. Phys.* **1979**, *71*, 381.
- (19) Montgomery, J. A. *Cancer Res.* **1959**, *19*, 447.
- (20) Broughton, B. J.; Chaplen, P.; Knowles, P.; Lunt, E.; Pain, D. L.; Wooldridge, K. R. H.; Ford, R.; Marshall, S.; Walker, J. L.; Marshall, D. R. *Nature* **1974**, *251*, 650.
- (21) Coulson, C. J.; Ford, R.; Lunt, E.; Marshall, S.; Pain, D. L.; Rogers, I. H.; Wooldridge, K. R. H. *Eur. J. Med. Chem.* **1974**, *9*, 313.
- (22) Raska, K., Jr.; Jurovcik, M.; Sormová, Z.; Sorm, F. *Collect. Czech. Chem. Commun.* **1965**, *30*, 3000.
- (23) Handschuhmacher, R. E.; Skoda, J.; Sorm, F. *Collect. Czech. Chem. Commun.* **1963**, *28*, 2983.
- (24) Kozłowski, D. L.; Singh, P.; Hodgson, D. J. *Acta Crystallogr., Sect. B* **1974**, *30*, 2806.
- (25) O'Donovan, P.; Perrett, C. M.; Zhang, X.; Montaner, B.; Xu, Y.-Z.; Harwood, C. A.; McGregor, J. M.; Walker, S. L.; Hanaoka, F.; Karran, P. *Science* **2005**, *309*, 1871.
- (26) Chen, M. S.; Chang, P. K.; Prusoff, W. H. *J. Biol. Chem.* **1976**, *251*, 6555.
- (27) Kittler, L.; Löber, G. *Photochem. Photobiol.* **1969**, *10*, 35.
- (28) Konishi, T.; Fujitsuka, M.; Luo, H.; Araki, Y.; Ito, O.; Chiang, L. Y. *Fullerenes, Nanot. Carbon Nanostruct.* **2003**, *11*, 237.
- (29) Martinez, L.; Martinez, C. G.; Klopotek, B. B.; Lang, J.; Neuner, A.; Braun, A. M.; Oliveros, E. *J. Photochem. Photobiol., B* **2000**, *58*, 94.
- (30) Miertus, S.; Scrocco, E.; Tomasi, J. *Chem. Phys.* **1981**, *55*, 117.
- (31) Barone, V.; Cossi, M.; Tomasi, J. *J. Comput. Chem.* **1998**, *19*, 404.
- (32) Frisch, M. J.; Trucks, G. W.; Schlegel, H. B.; Scuseria, G. E.; Robb, M. A.; Cheeseman, J. R.; Montgomery, J. A., Jr.; Vreven, T.; Kudin, K. N.; Buracilint, J. C.; Millam, J. M.; Iyengar, S. S.; Tomasi, J.; Barone, V.; Mennucci, B.; Cossi, M.; Scalmani, G.; Rega, N.; Petersson, G. A.; Nakatsuji, H.; Hada, M.; Ehara, M.; Toyota, K.; Fukuda, R.; Hasegawa, J.; Ishida, M.; Nakajima, T.; Honda, Y.; Kitao, O.; Nakai, H.; Klene, M.; Li, X.; Knox, J. E.; Hratchian, H. P.; Cross, J. B.; Bakken, V.; Adamo, C.; Jaramillo, J.; Gomperts, R.; Stratmann, R. E.; Yazyev, O.; Austin, A. J.; Cammi, R.; Pomelli, C.; Ochterski, J. W.; Ayala, P. Y.; Morokuma, K.; Voth, G. A.; Salvador, P.; Dannenberg, J. J.; Zakrzewski, V. G.; Dapprich, S.; Daniels, A. D.; Strain, M. C.; Farkas, O.; Malick, D. K.; Rabuck, A. D.; Raghavachari, K.; Foresman, J. B.; Ortiz, J. V.; Cui, Q.; Baboul, A. G.; Clifford, S.; Cioslowski, J.; Stefanov, B. B.; Liu, G.; Liashenko, A.; Piskorz, P.; Komaromi, I.; Martin, R. L.; Fox, D. J.; Keith, T.; Al-Laham, M. A.; Peng, C. Y.; Nanayakkara, A.; Challacombe, M.; Gill, P. M. W.; Johnson, B.; Chen, W.; Wong, M. W.; Gonzalez, C.; Pople, J. A. *Gaussian 03*, revision D.02; Gaussian, Inc.: Wallingford, CT, 2004.
- (33) Dennington, R.; Keith, T.; Millam, J.; Eppinnett, K.; Hovell, W. L.; Gilliland, R. *GaussView*, version 3.09; Semichem, Inc.: Shawnee Mission, KS, 2003.
- (34) Shemaker, A. L.; Hodgson, D. J. *J. Am. Chem. Soc.* **1977**, *99*, 4119.
- (35) Mmactintyre, W. M.; Singh, P.; Werkema, M. S. *Biophys. J.* **1965**, *5*, 697.
- (36) Singh, P.; Hodgson, D. J. *Acta Crystallogr.* **1974**, *B30*, 1430.
- (37) Parker, C. A.; Joyce, T. A. *Trans. Faraday Soc.* **1966**, *62*, 2785.
- (38) Wierzchowski, J.; Wielgus-Kutrowska, B.; Shugar, D. *Biochim. Biophys. Acta* **1996**, *1290*, 9.
- (39) Kobayashi, T.; Suzuki, T.; Ichimura, T.; Nanbu, S. To be submitted.
- (40) Murov, S. L.; Carmichael, I.; Hug, G. L. *Handbook of Photochemistry*, 2nd ed.; Marcel Dekker: New York, 1993.
- (41) Salet, C.; Bensasson, R. *Photochem. Photobiol.* **1975**, *22*, 231.